This article is published in *The Plant Cell* Online, *The Plant Cell* Preview Section, which publishes manuscripts accepted for publication after they have been edited and the authors have corrected proofs, but before the final, complete issue is published online. Early posting of articles reduces normal time to publication by several weeks.

Oscillatory Increases in Alkalinity Anticipate Growth and May Regulate Actin Dynamics in Pollen Tubes of Lily [W] [OA]

Alenka Lovy-Wheeler,[a] Joseph G. Kunkel,[a] Ellen G. Allwood,[b] Patrick J. Hussey,[b] and Peter K. Hepler[a,1]

[a] Department of Biology and Plant Biology Graduate Program, University of Massachusetts, Amherst, Massachusetts 01003
[b] Integrative Cell Biology Laboratory, Durham University, Durham DH1 3LE, United Kingdom

Lily (*Lilium formosanum* or *Lilium longiflorum*) pollen tubes, microinjected with a low concentration of the pH-sensitive dye bis-carboxyethyl carboxyfluorescein dextran, show oscillating pH changes in their apical domain relative to growth. An increase in pH in the apex precedes the fastest growth velocities, whereas a decline follows growth, suggesting a possible relationship between alkalinity and cell extension. A target for pH may be the actin cytoskeleton, because the apical cortical actin fringe resides in the same region as the alkaline band in lily pollen tubes and elongation requires actin polymerization. A pH-sensitive actin binding protein, actin-depolymerizing factor (ADF), together with actin-interacting protein (AIP) localize to the cortical actin fringe region. Modifying intracellular pH leads to reorganization of the actin cytoskeleton, especially in the apical domain. Acidification causes actin filament destabilization and inhibits growth by 80%. Upon complete growth inhibition, the actin fringe is the first actin cytoskeleton component to disappear. We propose that during normal growth, the pH increase in the alkaline band stimulates the fragmenting activity of ADF/AIP, which in turn generates more sites for actin polymerization. Increased actin polymerization supports faster growth rates and a proton influx, which inactivates ADF/AIP, decreases actin polymerization, and retards growth. As pH stabilizes and increases, the activity of ADF/AIP again increases, repeating the cycle of events.

INTRODUCTION

Proton concentration or pH regulates several important processes necessary for cell growth (Sze et al., 1999; Felle, 2001). In many cells, transmembrane pH gradients constitute prime energy transduction points that drive transport mechanisms. Proton concentrations can also affect enzyme activity (Guern et al., 1991), membrane trafficking (Caplan et al., 1987), endocytosis (Cosson et al., 1989), exocytosis (Gluck et al., 1982), and cytoskeletal stability (Andersland and Parthasarathy, 1993). Polarized cells, which must organize their structural components and metabolic activity in discrete domains to support unidirectional growth, are important objects for the study of pH gradients. For example, rhizoids of *Pelvetia* possess an intracellular pH gradient in their growing apex (Gibbon and Kropf, 1994). In root hairs (Bibikova et al., 1998), root caps (Fasano et al., 2001), and columella cells (Scott and Allen, 1999) of *Arabidopsis thaliana*, cytoplasmic pH changes are recognized as important signals that mediate directional growth and root gravity perception. Studies in animal cells also reveal that pH microdomains and actin polymerization play important roles in controlling cell polarity and growth (Bernstein et al., 2000; Bernstein and Bamburg, 2004; Ghosh et al., 2004).

The pollen tube is a particularly favorable system in which to study the existence and role of pH gradients in polarized growth because of its extremely rapid and highly focused tip extension. Prior work has already shown that these cells possess a marked proton gradient in their apical domain. Using bis-carboxyethyl carboxyfluorescein dextran (BCECF-dextran), together with ratiometric ion imaging, Feijó et al. (1999) revealed that lily pollen tubes possess an intracellular pH gradient in which the apex is slightly acidic, pH 6.8, whereas the subapex displays an alkaline band, pH 7.5. These gradients, however, are fragile, presumably because of high proton mobility. Thus, BCECF will dissipate pH microdomains when the dye concentration is 1 μM or greater (Feijó et al., 1999). The application of permeant buffers (Parton et al., 1997) or the injection of buffers such as HEPES (Feijó et al., 1999) emphasizes the importance of pH regulation, because these treatments dissipate local gradients and slow or inhibit pollen tube growth (Parton et al., 1997; Feijó et al., 1999). However, when growth is inhibited by other means, such as osmotic shock (Feijó et al., 1999), the alkaline band in the subapex of lily pollen tubes persists, whereas the acidic domain at the extreme apex disappears. This finding suggests that during growth inhibition the plasma membrane H^+-ATPases, which presumably produce the alkaline band, continue to function. The stimulation of proton ATPase activity and growth by fusicoccin and the inhibition by vanadate also support the idea that plasma membrane H^+-ATPases play a role in the maintenance of pH (Fricker et al., 1997).

Extracellular pH is also an important factor in regulating pollen tube growth. Acidic media are necessary, pH 4.5 to 6.5,

[1] To whom correspondence should be addressed. E-mail hepler@bio.umass.edu; fax 413-545-3243.
The author responsible for distribution of materials integral to the findings presented in this article in accordance with the policy described in the Instructions for Authors (www.plantcell.org) is: Peter K. Hepler (hepler@bio.umass.edu).
[W] Online version contains Web-only data.
[OA] Open Access articles can be viewed online without a subscription.
www.plantcell.org/cgi/doi/10.1105/tpc.106.044867

with pollen tube growth being inhibited at pH 7.0 or higher (Holdaway-Clarke et al., 2003). Also pertinent, growing pollen tubes show prominent extracellular fluxes of protons, with influx occurring at the extreme apex and efflux being localized along the sides of the apical dome, in a region occupied by the intracellular alkaline band (Feijó et al., 1999).

An important aspect of the intracellular and extracellular proton concentrations is that they oscillate during oscillatory growth. Within the cell, studies with BCECF-dextran indicate that both the alkaline band and the acidic apex oscillate (Feijó et al., 1999). In addition, Messerli and Robinson (1998), using c-SNARF-1, report the presence of oscillating acidic waves propagating from the apex. Finally, studies with the extracellular vibrating electrode reveal that the extracellular influx of protons into the apex oscillates (Feijó et al., 1999; Messerli et al., 1999). However, because of limitations in the signal, the establishment of the phase relationships of these ionic oscillations with growth has only been possible with the extracellular influx of protons and the intracellular proton waves. For these, cross-correlation analysis indicates that both follow growth by 7.5 s (Messerli and Robinson, 1998; Feijó et al., 1999). These following events thus respond to a preceding growth burst and therefore do not appear to cause the elongation process. To date, an ionic process leading growth has not been firmly established (Holdaway-Clarke and Hepler, 2003).

Together with the questions surrounding the properties of the pH gradients are those that focus on the role that these gradients play in growth. A potential target for pH in the growing pollen tube is the actin cytoskeleton. Actin in pollen tubes is abundant and forms domains of different structure; for example, in the apical region, F-actin forms a cortical fringe in which many bundles are

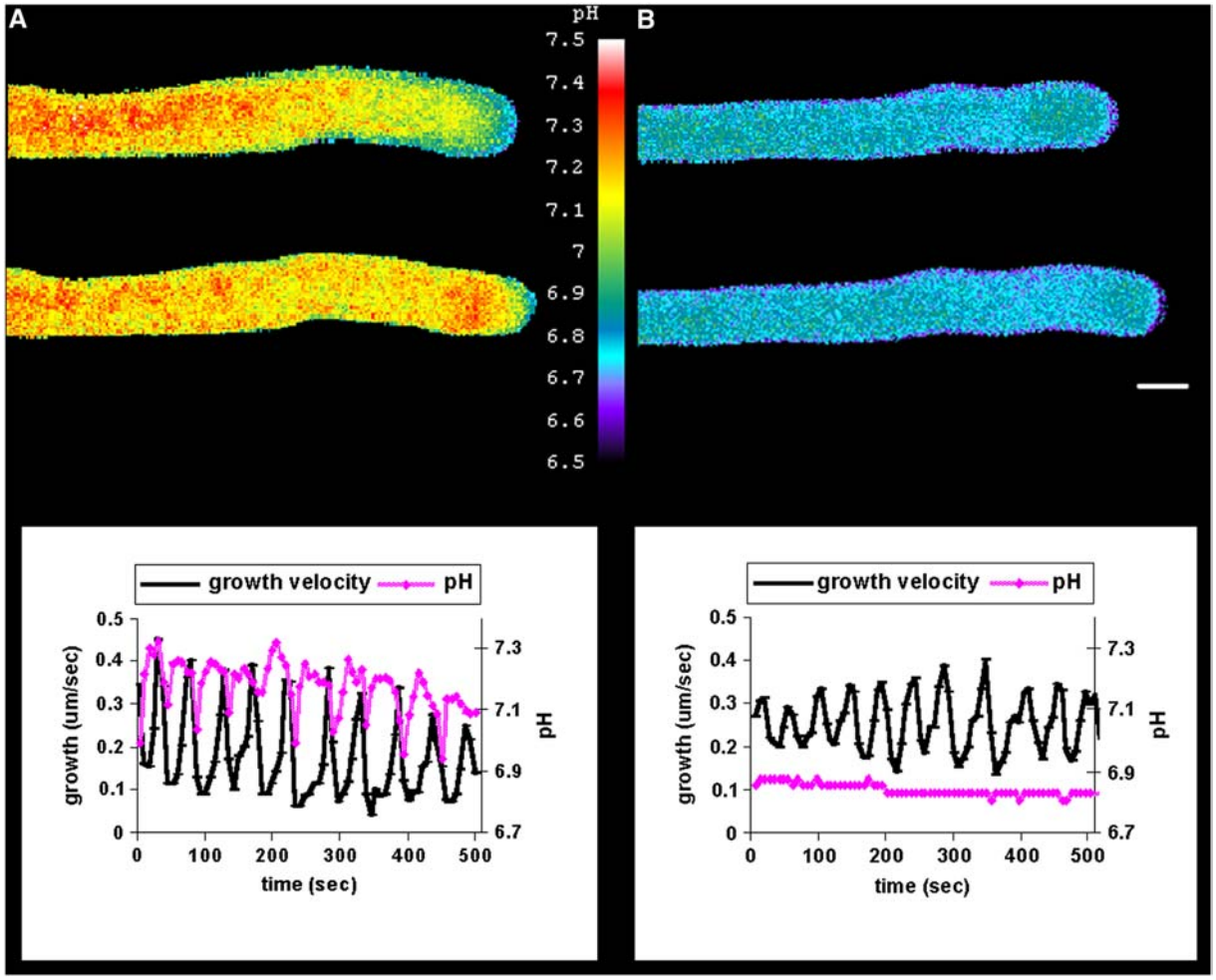

Figure 1. Changes in Intracellular pH during Oscillatory Pollen Tube Growth.

(A) Oscillating lily pollen tube injected with low levels of BCECF–70-kD dextran and subjected to ratiometric ion imaging. The corresponding graph of growth rate and pH change is shown at bottom. Measurements were taken at 7-s intervals within 20 μm of the apex. The pH changed by ~0.5 units in the apex.

(B) Oscillating lily pollen tube injected with low levels of a pH-insensitive rhodamine green dye and imaged with the same parameters (exposure time, binning, fluorescence range) as in **(A)**. The corresponding growth rate and pH change are shown at bottom.

Images were collected using wide-field fluorescence. Bar = 10 μm.

arranged parallel to the axis of growth (Lovy-Wheeler et al., 2005). It is noteworthy that this fringe of actin occupies the same domain as the alkaline band. Of further importance are several observations that support the idea that actin polymerization is necessary for pollen tube growth. Notably, actin-disrupting drugs inhibit growth at lower concentration than they inhibit cytoplasmic streaming, suggesting that actin polymerization may be linked to growth (Gibbon et al., 1999; Vidali et al., 2001). Live cell studies using green fluorescent protein (GFP)–talin to indirectly label the actin cytoskeleton indicate an oscillatory turnover of actin in the apex during growth (Fu et al., 2001). Additionally, the activity of RIC4, a ROP GTPase-interacting protein, which participates in actin regulation, oscillates in anticipation of growth and may control the process of actin polymerization (Gu et al., 2005; Hwang et al., 2005).

Although many actin binding proteins are likely involved in the control of actin dynamics of pollen tubes (Hussey et al., 2002), of particular pertinence to this study is actin-depolymerizing factor (ADF), because it responds to alkaline pH and stimulates actin turnover (Lopez et al., 1996; Gungabissoon et al., 1998; Allwood et al., 2002; Chen et al., 2002). In other systems, alkaline pH is thought to stimulate the fragmenting activity of ADF, yielding an increased number of actin plus ends and thus allowing more actin polymerization (Gungabissoon et al., 1998; Bernstein et al., 2000; Condeelis, 2001). For example, a photoactivatable form of ADF causes protrusions in keratocytes, identifying ADF activity as a prime controller of cell polarity (Ghosh et al., 2004). Recently, pollen-specific actin-interacting protein (AIP) has been identified and shown to enhance the depolymerization of F-actin in the presence of a pollen-specific ADF by ~60% in vitro (Allwood et al., 2002; Ketelaar et al., 2004a). Therefore, it seems plausible in the pollen tube that the alkaline band, by stimulating ADF/AIP, regulates actin polymerization and thus pollen tube growth.

Here, we have collected sequential data on pH oscillations and used cross-correlation analysis to compare their phase with growth rate oscillations in lily (*Lilium formosanum* or *Lilium longiflorum*) pollen tubes. We find that an increase in pH in the alkaline band leads the fastest growth rates, whereas acidification in the tip follows growth. ADF and AIP specifically localize to the actin fringe, and the modulation of intracellular pH profoundly alters the actin fringe as well as the distribution of ADF and AIP.

RESULTS

Apical pH Changes during Growth in Lily Pollen Tubes

Proton gradients that oscillate in growing pollen tubes of lily were routinely observed (Figure 1A). However, to make these observations, the final BCECF–10-kD dextran concentration in the cell must be <1 μM. These results are in close agreement with the previous report by Feijó et al. (1999). Although both studies were performed in the same laboratory, it is important to emphasize that a different microscope, CCD camera, and imaging software were used here than in the earlier study. Through the use of binning to increase camera sensitivity, we achieved repeatable (7-s) imaging of the pH gradient during oscillatory pollen tube growth. The results show a distinct oscillation in pH in the apical domain during oscillatory growth. Figure 1A shows an image of the change in pH commonly observed at low dye concentration. However, even at low concentration, we detected differences in the images depending on relatively small variations in the final dye concentration. Thus, when the concentration was 1 μM or less, the alkaline band and acidic tip were visible, as demonstrated by Feijó et al. (1999). Under these conditions, the most robust pH gradients were detected, spanning ~0.7 pH units, from pH 6.8 at the tip to pH 7.5 in the alkaline band. At somewhat higher dye levels (1 to 1.5 μM), the alkaline band was not as apparent, with several higher pH microdomains throughout the shank. Nevertheless, the most apparent pH gradients occurred in the apical domain. Under these conditions, the alkaline region was occasionally masked by a more dominant acidic influx, reminiscent of the acidic waves reported by Messerli and Robinson (1998). At even higher levels (>1.5 μM), the pH gradient was difficult to image. Nonoscillating pollen tubes did not exhibit significant changes in apical pH (data not shown), suggesting that oscillatory growth amplifies the pH changes enough for their imaging to be possible.

Although BCECF is a ratiometric dye that corrects for variations in dye concentration attributable to changes in accessible volume or local dye accumulation, we nevertheless were concerned about how well this would work at relatively low dye concentrations. Also, because elements of the endoplasmic reticulum flow into and out of the apical domain (Parton et al., 1997; Hepler et al., 2005) in an oscillatory pattern (Hepler et al., 2005), we thought that these may cause changes in the accessible volume that might affect dye behavior. To assess this potential problem, we injected pollen tubes with comparable levels of rhodamine green, which has the same excitation

Table 1. Cross-Correlation Analysis of Proton Concentration Minima and Maxima Versus Growth Rate

Growth Rate (μm/s)	Period (s)	Proton Minimum (s)	Proton Maximum (s)
0.25	70	−14	12
0.37	40	−10	12
0.10	30	−7	6
0.18	70	−22	15
0.12	30	−8	9
0.20	27	−10	5
0.30	37	−8	12
0.25	28	−14	1
0.28	49	−10	8
0.24	31	−12	2

The apical fluorescence of 10 pollen tubes injected with low levels of BCECF–70-kD dextran was measured over time and cross-correlated with growth rate. For each cell, the growth rate, period of growth oscillations, and time by which a particular pH characteristic leads (negative values) or lags (positive values) growth are displayed. The time shift presented for each cell is determined by calculating the highest correlation coefficient between two data sets consisting of at least seven oscillations. A pH increase (proton minimum) precedes the growth process, whereas a pH decrease (proton maximum) follows growth.

and emission spectrum as BCECF but which is insensitive to pH. Figure 1B shows an oscillating tube injected with rhodamine green (twofold to fourfold above background noise) and imaged with the same exposure times and the same image processing as used with BCECF. Although visually there is a slight lack of uniformity in the fluorescence signal in the apical domain, it does not exhibit an oscillation in intensity (Figure 1B). In further support of changes seen with BCECF, we tested other pH-sensitive dyes, including Oregon Green, SNARF, and pHluorin. All showed oscillations in proton concentration (data not shown); however, among these dyes, BCECF was the most effective.

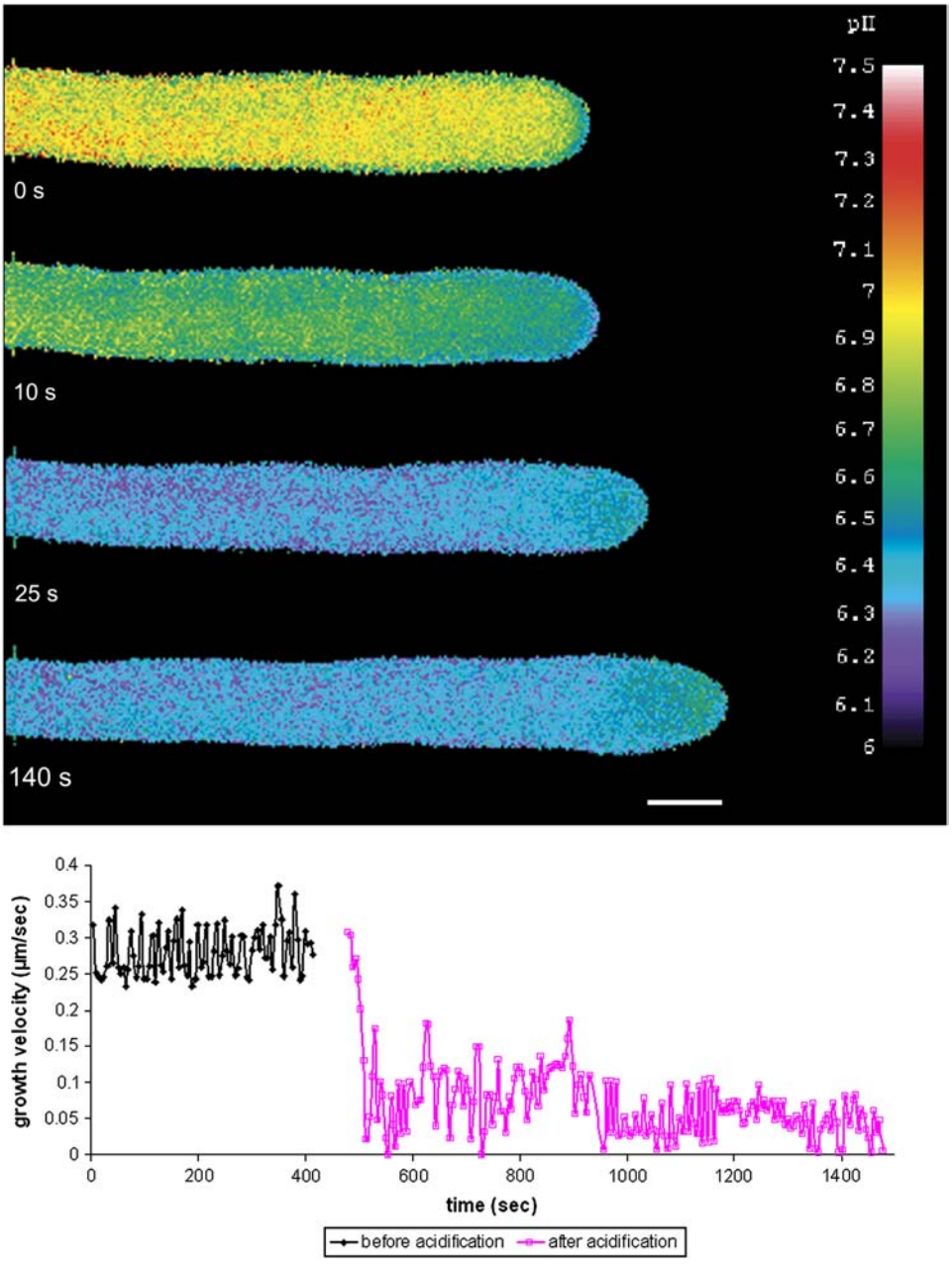

Figure 2. Intracellular Acidification of Lily Pollen Tubes with Sodium Acetate (10 mM).

A lily pollen tube was first injected with low levels of BCECF–70-kD dextran and then treated with 10 mM sodium acetate and imaged. The intracellular pH decreased to 6.3 within a few seconds, but the pollen tube continued to grow at ~20% normal growth rate. During this time, the alkaline band moved forward into the extreme apex and remained at higher pH (pH 6.8) than the rest of the pollen tube at pH 6.3 but lower than the usual alkalinity of pH 7.2 to 7.8 ($n = 5$). Images were collected using wide-field fluorescence. Bar = 10 μm. The bottom panel shows a graph of sustained but inhibited growth of pollen tubes.

Cross-Correlation Analysis of pH and Growth Oscillations

Given the oscillatory pattern of pH change relative to growth, these data were subjected to cross-correlation analysis. This analysis identifies whether a particular process is leading or lagging growth. If the process leads growth, there is a chance that its relationship to growth is causal, although this cannot be definitively determined. Cross-correlation analysis depends upon correlated regularities in change that exist between two oscillating measurements (Brillinger, 1981; Maindonald and Braun, 2003). Implementation of cross-correlation analysis also relies on irregularities in local wavelengths and the amplitudes of the two independent time series data sets to infer the direction of the phase offset. Despite the various appearances of pH oscillations at different dye levels, the quantification of the pH changes versus growth oscillations is consistent under minimal dye, and the oscillatory change can be described to have a general form. Table 1 expresses the proton concentration relative to growth in terms of a proton minimum (high pH) and proton maximum (low pH).

In the 10 pollen tubes measured, a pH increase (proton minimum) preceded a growth surge by an average of 11 s, and a pH decrease (proton maximum) lagged growth by an average of 8 s (Table 1). Each datum in Table 1 represents one cell exhibiting at least seven oscillations in both growth velocity and pH changes. Looking at the data more closely (graph in Figure 1A) reveals that the pH first increases quickly, then reaches a broad high point (proton minimum) before the next growth pulse. After the peak in growth there is brief, but dramatic, influx of protons (proton maximum) that causes a sharp decline in pH. Note that the pollen tube spends more time preparing for a growth surge, and this correlates with an increase in pH, indicating a possible link between the higher pH and growth velocity.

Effect of pH Modification on the Actin Fringe

The idea that actin polymerization is necessary for pollen tube growth (Gibbon et al., 1999; Vidali et al., 2001; Cárdenas et al., 2005) and the knowledge that the cortical actin fringe (Lovy-Wheeler et al., 2005) resides in the same region of the clear zone as the alkaline band (Feijó et al., 1999) suggest that pH might alter the actin cytoskeleton. First, the effects of acidification on pollen tube growth were determined. External treatment with 10 mM sodium acetate decreased the pH of the cytoplasm quickly by ~1 pH unit (Figure 2). Growth rates were inhibited by 80% for the first few minutes; however, within 10 to 15 min, growth stopped completely. The clear zone became shorter, the alkaline band moved into the tip, and the acidic tip could no longer be detected. This condition could be reversed: if growth inhibition was not prolonged (>10 min), a return to normal conditions allowed complete recovery.

Next, the structure of actin in acidified cells was examined by two methods described by Lovy-Wheeler et al. (2005). One method involves chemical fixation and phalloidin staining. Control cells showed the actin cortical fringe in the apex of the pollen tube, and long actin bundles dispersed throughout the shank (Figure 3A). Acidification of the cytoplasm with 10 mM sodium acetate for 30 s rendered the actin fringe in the apex less robust and broke down many of the actin bundles throughout the shank (23 of 30 cells; Figure 3B). Interestingly, the actin fringe moved into the apex of the pollen tube, as did the alkaline region, further supporting the idea that these two cellular features are interrelated and that this is a region where actin polymerization occurs. It should be pointed out that this alkaline region in acidified cells is lower in pH than the alkaline band of normal cells but is a region of highest pH in acidified cells. When pollen tubes were treated with high concentrations of sodium acetate (100 mM) and chemically fixed within 5 to 15 s, the actin fringe was completely degraded, whereas the actin filaments in the shank of the pollen tube still remained, indicating the high sensitivity of the cortical actin fringe (Figure 3C). The pH of the growth medium was unaltered in the 10 mM sodium acetate solution and increased to pH 6.0 at

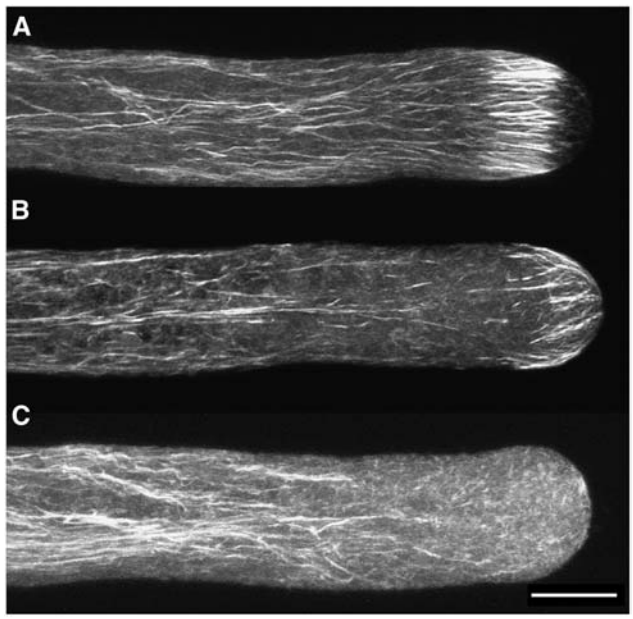

Figure 3. Effect of Intracellular Acidification on the Actin Cytoskeleton as Revealed by Chemical Fixation and Phalloidin Staining.

(A) Control lily pollen tube chemically fixed with EGS and stained with phalloidin. The actin cytoskeleton is organized in long bundles parallel to the long axis of the pollen tube, with a prominent cortical actin fringe at the apex as described previously (Lovy-Wheeler et al., 2005).

(B) Lily pollen tube acidified with 10 mM sodium acetate. After this treatment, which inhibits growth by 80% ($n = 5$), cells were fixed chemically after 30 s with ethylene glycol bis[sulfosuccinimidyl succinate] (sulfo-EGS) and stained with phalloidin. The actin cytoskeleton is less robust, but some of the actin fringe remains and is positioned closer to the apex than usual (23 of 30 cells).

(C) Lily pollen tube acidified with 100 mM sodium acetate, chemically fixed with EGS within 15 s, and stained with phalloidin ($n = 10$). The cortical actin fringe is the first to disappear when pollen tube growth is inhibited by rapid acidification. Filaments in the shank remain relatively undisturbed in this short time frame.

Images are projections of confocal laser scanning microscopy (CLSM) slices collected every 1 μm. Bar = 10 μm.

100 mM sodium acetate, still within the normal range to support pollen tube growth (Holdaway-Clarke et al., 2003).

We recognize that it would be best if we could visualize these actin changes in live cells; however, there are significant problems. First, to the best of our knowledge, a reliable actin probe does not yet exist in plants. Expression levels of actin binding GFP chimeras have to be strictly monitored to avoid misinterpretation of data (Ketelaar et al., 2004b). To date, only fluorescently tagged actin binding proteins are available (Kost et al., 1998; Chen et al., 2002; Wang et al., 2004), and these only indirectly reveal the structure of actin. Second, as noted in a recent study (Wilsen et al., 2006), it has not been possible to routinely label the cortical actin fringe in lily pollen tubes. When it is labeled, it still lacks the clarity and definition of cryofixed or sulfo-EGS–fixed samples. Cryofixation permits the use of antibodies (Lovy-Wheeler et al., 2005); therefore, we used this method to study actin as well as two actin binding proteins, ADF and AIP.

Plunge-freeze fixation followed by freeze substitution, rehydration, and antibody labeling showed similar, but not identical, results as the chemical fixation procedure (Figure 4). Under control conditions, the actin fringe was as clear and robust as shown by Lovy-Wheeler et al. (2005) (Figure 4A). However, when the pollen tubes were treated with 10 mM sodium acetate for 30 s, the actin filaments in the cortical fringe were greatly reduced and the antibody staining accumulated in the apex (Figure 4B). In this regard, the plunge-frozen, actin antibody–labeled cells were different from those fixed with sulfo-EGS and labeled with phalloidin. The reason for this, we believe, is that phalloidin stains only F-actin, whereas the antibody stains both F- and G-actin. Because of the marked increase in G-actin, its staining masks the microfilaments that remain.

Alkalinizing the cytoplasm of pollen tubes proved to be more difficult than acidification. We tried different ammonia reagents reported previously to increase the cellular pH but could not achieve an increase that persisted long enough without abolishing growth to examine alkaline effects on the structure of the actin fringe. Treatment with 10 μM fusicoccin did transiently increase the cytosolic pH (Figure 5), but pollen tubes quickly reequilibrated to normal pH levels. When we examined the actin cytoskeleton after a brief treatment with 10 μM fusicoccin, using EGS chemical fixation, no effect could be detected relative to controls ($n = 100$). Additionally, there was no consistent effect of fusicoccin on pollen tube growth ($n = 2500$) or growth oscillations ($n = 10$) (data not shown). In some instances, the growth velocity of weak pollen tubes was stimulated by fusicoccin, but this effect could not be observed consistently.

When pollen tubes were treated with growth medium at pH 8, in an attempt to increase intracellular pH, growth was inhibited without an effect on cytoplasmic streaming, as observed previously (Holdaway-Clarke et al., 2003). Although the pH of the pollen tubes increased slightly (0.1 unit), the effect was not consistent. However, the pH became uniform from the tip to the shank. Under these conditions, the actin fringe disintegrated; shorter mesh-like actin filaments remained in the apex, whereas the filaments in the shank appeared as usual (Figure 6B). These results were similar to the growth inhibition by higher concentrations of sodium acetate (Figure 3C), in which the actin fringe degraded concomitantly with growth inhibition; actin bundles in the shank of the tube remained and supported cytoplasmic streaming.

Localization of ADF and AIP

A candidate binding protein that controls actin dynamics in pollen tubes is ADF. Pollen ADF activity increases at more alkaline pH values (Gungabissoon et al., 1998; Allwood et al., 2002; Chen et al., 2002) and thus is likely to stimulate actin turnover in the region of the alkaline band, where the cortical actin fringe resides. AIP increases ADF activity by 60%; therefore, it is of interest to examine the localization of both proteins (Allwood et al., 2002). In prior work, it was shown that ADF and

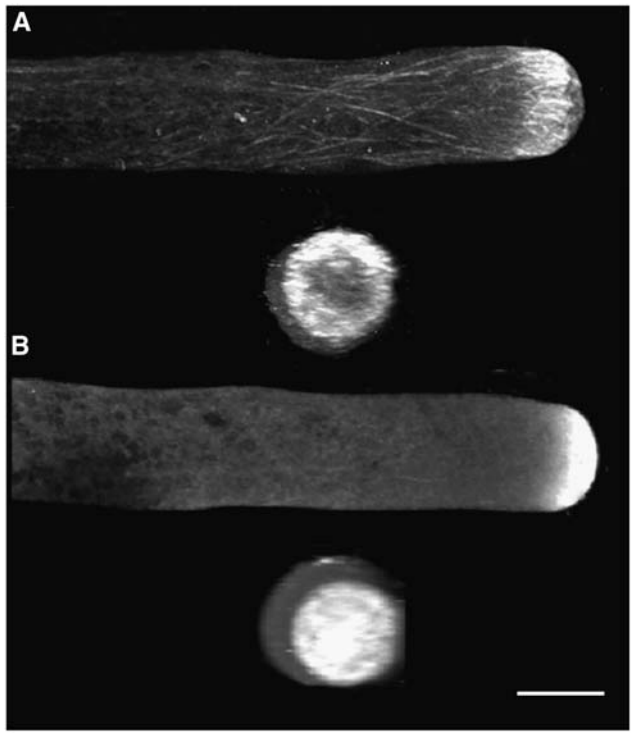

Figure 4. Effect of Intracellular Acidification on the Actin Cytoskeleton as Revealed by Rapid Freeze-Fixation and Immunolabeling.

(A) Control lily pollen tube plunge-frozen, freeze-substituted, rehydrated, and immunolabeled for actin. The actin cytoskeleton is organized in long actin bundles parallel to the long axis of the pollen tube, with a prominent cortical actin fringe in the apical region as shown previously (Lovy-Wheeler et al., 2005).

(B) Lily pollen tube acidified with 10 mM sodium acetate for 30 s and then plunge-frozen and processed for whole mount actin immunolabeling. The actin cables in the shank diminish, and the cortical actin fringe disappears. Actin antibodies prominently label the apex of the pollen tube, presumably corresponding to G-actin generated by the breakdown of the actin fringe ($n = 20$). Also note that after acidification, the fibrillar nature of the fringe is not evident.

Images are projections of CLSM slices collected every 1 μm. Bar = 10 μm.

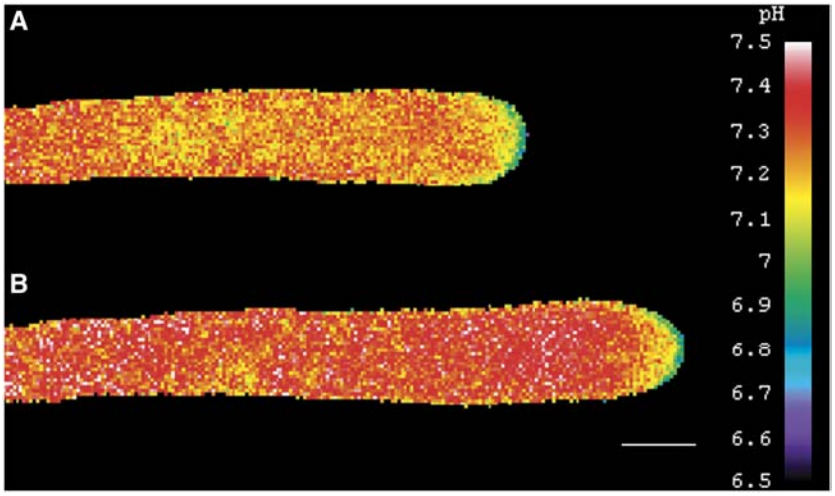

Figure 5. Intracellular Alkalinization Using 10 μM Fusicoccin.

(A) A lily pollen tube was injected with low levels of BCECF–70-kD dextran and treated with 10 μM fusicoccin before treatment.
(B) One minute after addition of 10 μM fusicoccin. The pH increases slightly but quickly equilibrates to original values ($n = 10$).
Images were collected by wide-field fluorescence. Bar = 10 μm.

AIP localize similarly; however, the procedures used in that study were not optimized to also image the cortical actin fringe (Allwood et al., 2002). For this reason, we were interested in applying the newly developed whole mount procedure to localize ADF and AIP. Figure 7 shows that ADF and AIP localized to a cortical ring at the apex of the pollen tube, in the same location as the cortical actin fringe. ADF was mostly concentrated at the apex, with some signal also dispersed throughout the shank (Figure 7A). AIP showed a prominent cortical ring at the apex but was also dispersed throughout the cytoplasm in the pollen tube shank (Figure 7C).

After acidification for 30 s with 10 mM sodium acetate, both proteins moved into the tip of the pollen tube and no longer formed a cortical label as in controls (seven of seven cells, Figure 7B; three of five cells, Figure 7D). A similar situation occurred in an acidified pollen tube; thus, we presume that ADF and AIP labeling depends on the actin fringe. When pollen tubes were acidified for longer periods of time, the localization of ADF and AIP disappeared from the apex. This was probably a result of ongoing cytoplasmic streaming in these growth-inhibited cells, which in the absence of the actin fringe would eventually disperse proteins that heretofore had bound to the fringe. Double labeling experiments with actin and ADF or AIP are challenging because both antibodies originate from mouse. However, from the observation that ADF and AIP became disrupted similarly to actin during cytoplasmic acidification, we assume that these proteins are normally associated with the actin fringe.

DISCUSSION

Our results provide evidence that changes in intracellular pH constitute a potential central regulator of oscillatory pollen tube growth. The data clearly show an oscillation in pH that correlates with an oscillation of similar period in the growth rate. When these two oscillatory patterns are subjected to cross-correlation analysis to decipher their phase relationship, the results reveal that the increase in alkalinity anticipates the increase in growth rate, whereas the increase in acidity follows growth. For several reasons, we suggest that the anticipatory pH increase modulates growth through its effect on the actin cytoskeleton. First, the alkaline zone corresponds spatially with the localization of the cortical actin fringe as well as two crucial actin binding proteins, ADF and AIP, in the apical domain. Second, ADF is a pH-sensitive actin binding protein whose ability to simulate actin

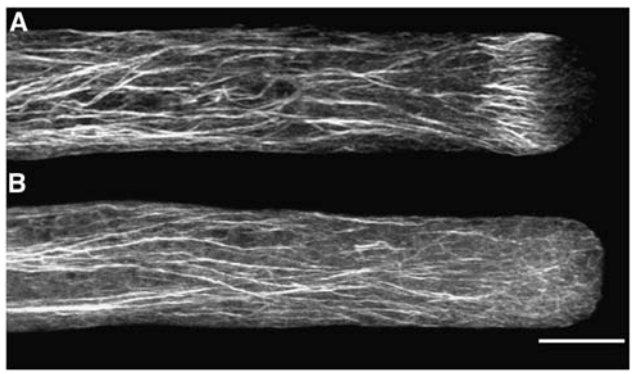

Figure 6. Effect of Alkaline Condition on Actin Structure.

(A) Control lily pollen tube chemically fixed with EGS and stained with phalloidin.
(B) Lily pollen tube after 1-min treatment with pH 8.0 buffer, fixed and stained as in **(A)**. Pollen tubes lose the cortical actin fringe simultaneously with the inhibition of growth. Although pollen tube growth was inhibited, cytoplasmic streaming continued for several minutes after treatment. The apex now contains more of a meshwork of actin filaments. The actin filaments in the shank appear normal ($n = 10$).
Images are projections of CLSM slices taken every 1 μm. Bar = 10 μm.

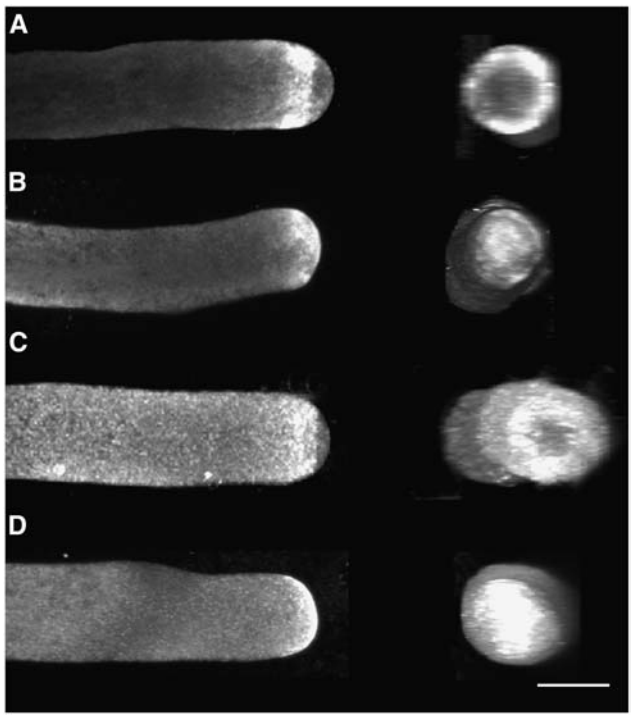

Figure 7. Effect of Intracellular Acidification on the Localization of the Actin Binding Proteins ADF and AIP.

(A) Control lily pollen tube plunge-frozen and processed for whole mount immunolabeling with lily-specific ADF antibodies. Lily ADF labels a cortical fringe in the apex of the pollen tube, in the same vicinity as the cortical actin fringe ($n = 10$).

(B) Lily pollen tube acidified with 10 mM sodium acetate for 30 s, then plunge-frozen and immunolabeled with lily-specific ADF antibodies. ADF moves forward into the apex of the pollen tube (seven of seven cells). This labeling looks similar to actin immunolabeling after intracellular acidification.

(C) Control lily pollen tube plunge-frozen and processed for whole mount immunolabeling with AIP antibodies. AIP predominantly labels a cortical ring in the apex of the pollen tube but is also spread throughout the shank of the tube ($n = 10$).

(D) Lily pollen tube acidified with 10 mM sodium acetate for 30 s, then plunge-frozen and immunolabeled with AIP antibodies. AIP moves into the apical region of pollen tubes, as occurs with actin immunolabeling upon intracellular acidification (three of five cells).

Images are projections of CLSM slices taken every 1 μm. Bar = 10 μm.

turnover is enhanced by an increase in pH and by the presence of AIP. Finally, experimental induction of cytoplasmic acidification markedly slows pollen tube growth while simultaneously destroying the cortical actin fringe. Thus, it seems plausible that an increase in alkalinity stimulates ADF to fragment F-actin in the cortical fringe. The fragmentation exposes new plus or barbed ends that in turn enhance new polymerization of actin, which is necessary to support pollen tube growth. Although the research associated with this study has focused on the relationship between pH and the actin cytoskeleton, we realize that pH may cause profound changes in energy metabolism and that these may also play a key role in controlling pollen tube growth.

The abrupt acidification event, which closely follows growth, may enhance a variety of processes that contribute to a slowing of growth. The magnitude of the detected pH change ranges from 6.8 to 7.5, which constitutes a change in proton concentration of approximately fivefold. Messerli and Robinson (1998) have focused on the acidification process and suggest, as a follower of growth, that it may play a key role in downregulating calcium binding proteins, slowing secretion, and thus contributing to the slowing of growth. It also seems clear that the decrease in pH will inactivate ADF and thus retard the actin turnover that is necessary for pollen tube growth.

Of note is the asymmetry of the growth oscillations and pH oscillations, in which the pH initially increases quickly and then more slowly forms a plateau. It is during this time that the growth velocity reaches its peak (Figure 1A). However, once at maximal growth velocity, the proton concentration changes rapidly and the growth rate declines concomitantly. Although both alkalinization and acidification are closely related, we suggest that they are caused by two distinct events. The increase in pH presumably is attributable to the activity of a proton ATPase located on the plasma membrane (see below). By contrast, the proton influx, which accounts for the acidification, may result from a growth-dependent opening of a cation channel on the apical plasma membrane. Although proton influx in tip-growing fungal hyphae (*Achlya*) has been shown to be associated with the symport of amino acids (Harold and Caldwell, 1990), we do not think that this process is a factor in pollen tubes, because pollen tubes do not require amino acids in their growth medium. More importantly, proton influx displays similar characteristics to that for calcium: in pollen tubes, both ions exclusively enter the extreme apex and show the same lag from growth. Therefore, it is attractive to suggest that protons enter a stretch-activated channel at the apex. Dutta and Robinson (2004) have described such a stretch channel that appears to respond to growth and allow the entry of calcium ions. Here, we suggest that protons enter the same channel, or a similarly activated channel. Although calcium itself occupies an important position in the regulation of pollen tube growth, the broad outlines can be explained simply through a consideration of proton activity. In brief, an oscillatory sequence of events emerges as follows: alkalinity promotes growth; growth promotes proton influx; protons negatively affect growth. pH gradients are driven by H^+-ATPases that occur on the plasma membrane of plant cells (for reviews, see Sze et al., 1999; Palmgren, 2001). In pollen tubes, localization studies indicate that these enzymes reside on pollen grains (Feijó et al., 1992; Obermeyer et al., 1992) but also along the tube itself. More recent studies using GFP fusion indicate a distinct localization along the entire pollen tube plasma membrane, with the exception of the extreme apex, where the H^+-ATPase is conspicuously absent (Lefebvre et al., 2005). Additional evidence for a localized activity of this H^+-ATPase derives from studies with the extracellular proton-selective probe, which indicate proton effluxes along the shank of the pollen tube. It is reasonable to assume that the H^+-ATPases generate both the alkaline band on the inside of the cell and the H^+ flux observed on the outside of the cell (Feijó et al., 1999). Whether or not this enzyme oscillates in activity is not known. However, the observations with the proton-specific extracellular electrode that show oscillations of influx at the tip

but no oscillations of efflux along the shank are consistent with the view that the enzyme activity is steady and nonoscillatory. Perhaps it is the influx of protons caused by oscillatory growth that causes the pH to oscillate, whereas the proton ATPase activity is relatively constant.

Experimental modification of pH using permeant buffers, while providing some interesting results, is nevertheless fraught with problems, in large measure because the effects are global and not directed at modifying events in the apical domain. Even so, the results clearly show that acidification quickly destroys the apical actin fringe without impairing the actin cables in the shank of the tube. Controlled alkalinization has been difficult to achieve. With fusicoccin, we observed a brief increase in pH, but this quickly equilibrated. Therefore, we have not been able to observe the effect of an imposed alkalinization on the cortical actin fringe.

Although we have focused on the regulation of actin by pH, it is possible that actin, together with actin binding proteins, plays a role in depositing or forming a complex with H^+-ATPases at the cortical fringe. This scenario would be analogous to the situation in fibroblasts, in which a Na-H exchanger (NHE1) has been shown to function as an anchor for actin through ezrin/radixin/moesin proteins (Denker and Barber, 2002). Possibly, a similar situation occurs in the cortical actin fringe of the pollen tube. Although homologs of ezrin/radixin/moesin anchoring proteins have not been identified in pollen tubes, similarly functioning actin binding proteins might be present that create a link between the H^+-ATPase on the plasma membrane and the actin in the cortical fringe.

Although the focus here has been on pH oscillations, calcium oscillations are also prominent in the pollen tube apex, and these, either directly or together with pH oscillations, affect actin polymerization or activity through actin binding proteins such as myosin (Yokota et al., 1999), profilin (Kovar et al., 2000), villin (Yokota et al., 2005), and gelsolin (Fan et al., 2004; Huang et al., 2004). For example, profilin, in regions of high calcium, such as the apex, demonstrates a much reduced ability to support actin polymerization (Kovar et al., 2000). Villin, which bundles actin at basal levels of calcium, in the presence of high calcium and calmodulin, unbundles actin filaments (Yokota et al., 2005). A related protein, gelsolin, was recently identified in pollen tubes, and this effectively fragments F-actin in regions of increased calcium (Fan et al., 2004; Huang et al., 2004). Finally, myosin XI, the common motor protein responsible for streaming in pollen tubes, is downregulated by increased calcium (Yokota et al., 1999). Therefore, it should be evident that calcium plays an important role in the control of actin structure and function in the pollen tube apex; it should also be apparent that as the calcium oscillates, these associated effects on actin will also oscillate. It

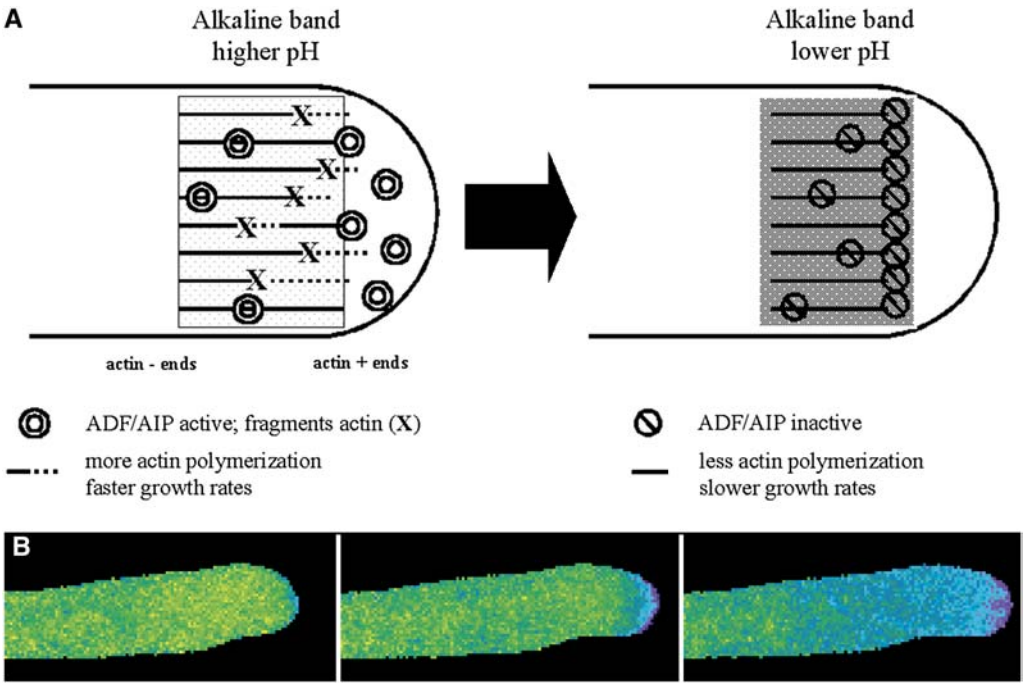

Figure 8. Hypothetical Model of How pH May Affect Actin through ADF/AIP.

(A) As the pH increases, the activity of ADF/AIP increases, leading to the fragmentation of existing actin filaments, which exposes a greater number of barbed ends. These actin plus ends stimulate polymerization, which in turn stimulates growth rates and leads to a wave of proton influx. The decrease in pH inactivates ADF/AIP, which reduces actin polymerization and the growth rate. The cycle repeats itself when the pH in the alkaline band starts to increase, reactivating ADF/AIP.

(B) Three sequential images from the Supplemental Movie online illustrating cytoplasmic pH changes in a lily pollen tube merged with a sonic representation of three events: maximal pH, maximal growth rate, and minimal pH.

is further likely that calcium and protons work together to achieve their effects. For example, as noted previously, the entry of both ions follows growth by a few seconds and may be attributable to passage through stretch-activated channels (Dutta and Robinson, 2004). Their simultaneous increase collectively ensures that actin polymerization in the apex will be vigorously inhibited, in a process that would be expected to contribute to the decline in growth rate.

For the results presented in this study, we provide a summary model (Figure 8). We propose that the anticipatory increase in pH stimulates ADF/AIP and that these proteins fragment existing F-actin in the cortical fringe. The fragmentation exposes more plus ends, which then stimulates actin polymerization and faster growth rates. As the growth rate increases, the deformation of the apical plasma membrane opens stretch-activated channels, which allow the entry of protons (and calcium). The resulting acidification inactivates ADF/AIP, decreases actin polymerization, and retards growth. As the protons dissipate, the pH increases steadily and the cycle starts all over again.

METHODS

Cell Culture

Lilium formosanum and *Lilium longiflorum* were grown in a medium containing 15 mM MES, 1.6 mM HBO_3, 1 mM KCl, 0.1 mM $CaCl_2$, and 7% sucrose, pH 5.5. For plunge-freezing, the level of sucrose was increased to 10%. Unless stated otherwise, all chemicals were purchased from Sigma-Aldrich.

Cytosolic pH Ratiometric Imaging

L. formosanum pollen tubes were pressure-injected with 0.1 mg/mL BCECF–70-kD dextran (Molecular Probes) using microneedles pulled in a vertical pipette puller (model 700D; David Kopf Instruments) from borosilicate glass capillaries (World Precision Instruments). Pollen tubes were illuminated with two excitation wavelengths, 440/20 nm bandwidth (reference) and 495/10 nm bandwidth (pH-dependent) generated by a xenon bulb (DG-4; Sutter Instruments), and sequentially imaged every 7 s. Although the amount of dye injected could not be tightly controlled, we attempted to work with dye levels below the dye-buffering range of 1 μM. The total dye concentration in the cell was estimated by quantifying the fluorescence emission of the independent channel (440 nm) as described previously (Feijó et al., 1999). The application of 4 μL of dye on an 18-mm cover slip forms a 16-μm layer of dye, which roughly corresponds to the thickness of lily pollen tubes. The calibration curve assured us that we were working in the appropriate dye range. All filters including the emission filter (535/25 nm) were purchased from Chroma Technology. Images were collected with a charge-coupled device camera (Quantix Cool Snap HQ; Roper Scientific) attached to a Nikon TE300 inverted microscope (Nikon Instruments) using a ×40, 1.3 numerical aperture oil-immersion objective lens operated with MetaMorph/MetaFluor software (Universal Imaging). Images were binned (3 × 3) to improve the signal above background. In vitro calibrations were performed using BCECF–70-kD dextran in a pseudocytosol medium (Poenie, 1990; Feijó et al., 1999) composed of 100 mM KCl, 30 mM NaCl, 500 mM mannitol, 40% sucrose, 25 mM MES, and 25 mM HEPES adjusted to pH 6.3, 6.5, 6.7, 6.9, 7.1, 7.3, 7.5, and 7.8.

Experimental acidification was achieved by treating cells with 10 and 100 mM sodium acetate (Tsai et al., 1995). Sodium acetate (100 mM) was usually applied for periods of 5 to 15 s, whereas 10 mM sodium acetate was applied for 30 s. Alkalinization was achieved by treatment with 10 μM fusicoccin diluted in germination medium. Inhibition of growth was achieved with standard germination medium at pH 8.

Cross-Correlation Studies

Measurements of fluorescence representing proton concentration changes were made by placing 29 square regions (~3 × 3 μm) within the lily pollen tube apex and monitoring the changes within these regions over time. The relative positions of the 29 regions at the tip of the pollen tube remained constant. Because the regions within the 20-μm area from the tip all exhibited similar temporal values of changing fluorescence, we report values from just one box in the vicinity of the actin fringe. Application of cross-correlation analysis depends on a periodicity in the waveform of both the growth rate and pH versus time. Because of small variation in the period and amplitude of these two waveforms, the process of cross-correlation reveals a better fit when shifted in one direction relative to the other. The direction of better fit thus provides evidence on whether the pH increases before or after maximal growth rates. Two independent measures can thus be correlated, and the phase delay between the two time series processes can be deciphered (Brillinger, 1981). Oscillatory profiles of growth velocities and pH values were cross-correlated using the convolution function from the stats library of the R computational environment (Maindonald and Braun, 2003). Growth velocities and pH changes were subjected to a Lowess smoothing function to achieve baseline correction (Cleveland, 1981).

Cryofixation/Immunolabeling

L. longiflorum was surface-germinated on pollen tube growth medium for 2 to 4 h, picked up on 3% agar loops, and plunge-frozen as described (Lancelle et al., 1986). Pollen tubes were freeze-substituted at −80°C for 36 h in dry acetone but supplemented with 2 to 5% anhydrous glutaraldehyde. Samples were placed in a precooled −80°C metal block and allowed to come to room temperature over a period of 8 h. The loops containing the pollen tubes were rehydrated in 10% steps (15 to 30 min each) to 100% water and then placed into 10 mM PBS. Pollen tubes were treated with 0.1% $NaBH_4$ for 15 min and then rinsed with PBS supplemented with 0.1% (w/v) Tween 20 for 15 min. Monoclonal mouse anti-actin antibody (C4 raised against chicken gizzard actin; Chemicon), mouse anti-LIADF1, or mouse anti-AtAIP1 was applied at 4°C overnight and washed six times in PBS supplemented with 0.05% (w/v) Tween 20, and secondary goat anti-mouse Cy3 antibody (Jackson Immunoresearch Laboratories) was applied for 3 to 4 h at 37°C. Pollen tubes were washed six times with 0.05% Tween 20 and PBS for 5 min each and mounted in 4% *n*-propyl gallate (90% glycerol and 10% PBS) (for details, see Lovy-Wheeler et al., 2005).

Imaging was performed on a Carl Zeiss LSM510 Meta confocal microscope using the HeNe 543-nm excitation laser and a long-pass 568-nm emission filter.

Chemical Fixation

L. formosanum or *L. longiflorum* pollen tubes were cultured for 1 to 2 h and simultaneously fixed and permeabilized with a buffer composed of 100 mM PIPES, 5 mM $MgSO_4$, 0.5 mM $CaCl_2$, 0.05% Triton X-100, 1.5% formaldehyde, and 0.05% glutaraldehyde, pH 9.0, for 0.5 h. EGS was added at 5 mM. The growth medium was completely removed before adding the fixative. The fixative was removed, and the cells were washed once with the same buffer described above except at pH 7.0 with 10 mM EGTA and 6.6 μM (10 μL/mL) Alexa 488–phalloidin (Molecular Probes) (Lovy-Wheeler et al., 2005). Images could be taken as early as 15 min, but the best results were obtained at 1 to 2 h after staining. Imaging (CLSM) was performed on a Zeiss LSM510 Meta confocal microscope using the argon 488-nm excitation laser and a long-pass 505-nm emission filter.

Supplemental Data

The following material is available in the online version of this article.

Supplemental Movie 1. Simultaneous Visual and Sonic Representation of pH Changes and Growth Rate in a Lily Pollen Tube.

ACKNOWLEDGMENTS

We thank our colleagues at the University of Massachusetts for their helpful suggestions during the preparation of this study. We thank composer and computer music specialist Matt Waugh for representing biological events sonically. We also thank the Central Microscopy Facility for the use of the laser scanning confocal microscope and acknowledge its supporting grant from the National Science Foundation (Grant NSF BBS 8714235). We thank the Davis and DeLisle Funds of the Plant Biology Graduate Program for their contribution. This project was supported by National Science Foundation Grants MCB-0077599 and MCB-0516852 to P.K.H.

Received June 13, 2006; revised July 14, 2006; accepted July 26, 2006; published August 18, 2006.

REFERENCES

Allwood, E., Anthony, R., Smertenko, A., Reichelt, S., Drøbak, B., Doonan, J., Weeds, A., and Hussey, P. (2002). Regulation of the pollen-specific actin-depolymerizing factor LlADF1. Plant Cell **14,** 2915–2927.

Andersland, J.M., and Parthasarathy, M.V. (1993). Conditions affecting depolymerization of actin in plant homogenates. J. Cell Sci. **104,** 1273–1279.

Bernstein, B., and Bamburg, J. (2004). A proposed mechanism for cell polarization with no external cues. Cell Motil. Cytoskeleton **58,** 96–103.

Bernstein, B.W., Painter, W.B., Chen, H., Minamide, L.S., Abe, H., and Bamburg, J.R. (2000). Intracellular pH modulation of ADF/cofilin proteins. Cell Motil. Cytoskeleton **47,** 319–336.

Bibikova, T.N., Jacob, T., Dahse, I., and Gilroy, S. (1998). Localized changes in apoplastic and cytoplasmic pH are associated with root hair development in *Arabidopsis thaliana.* Development **125,** 2925–2934.

Brillinger, D. (1981). Time Series: Data Analysis and Theory. (San Francisco, CA: Holden-Day).

Caplan, M.J., Stow, J.L., Newman, A.P., Madri, J., Anderson, H.C., Farquhar, M.G., Palade, G.E., and Jamieson, J.D. (1987). Dependence on pH of polarized sorting of secreted proteins. Nature **329,** 632–635.

Cárdenas, L., Lovy-Wheeler, A., Wilsen, K.L., and Hepler, P.K. (2005). Actin polymerization promotes the reversal of streaming in the apex of pollen tubes. Cell Motil. Cytoskeleton **61,** 112–127.

Chen, C., Wong, E., Vidali, L., Estavillo, A., Hepler, P., Wu, H.-M., and Cheung, A. (2002). The regulation of actin organization by actin-depolymerizing factor in elongating pollen tubes. Plant Cell **14,** 2175–2190.

Cleveland, W. (1981). Lowess—A program for smoothing scatterplots by robust locally weighted regression. Am. Stat. **35,** 54.

Condeelis, J. (2001). How is actin polymerization nucleated *in vivo*? Trends Cell Biol. **11,** 288–293.

Cosson, P., Decurtis, I., Pouyssegur, J., Griffiths, G., and Davoust, J. (1989). Low cytoplasmic pH inhibits endocytosis and transport from the trans-Golgi network to the cell surface. J. Cell Biol. **108,** 377–387.

Denker, S.P., and Barber, D.L. (2002). Cell migration requires both ion translocation and cytoskeletal anchoring by the Na-H exchanger NHE1. J. Cell Biol. **159,** 1087–1096.

Dutta, R., and Robinson, K.R. (2004). Identification and characterization of stretch-activated ion channels in pollen protoplasts. Plant Physiol. **135,** 1398–1406.

Fan, X., Hou, J., Chen, X., Chaudhry, F., Staiger, C., and Ren, H. (2004). Identification and characterization of a Ca^{2+}-dependent actin filament-severing protein from lily pollen. Plant Physiol. **136,** 3979–3989.

Fasano, J., Swanson, S., Blancaflor, E., Dowd, P., Kao, T.-H., and Gilroy, S. (2001). Changes in root cap pH are required for the gravity response of the *Arabidopsis* root. Plant Cell **13,** 907–922.

Feijó, J.A., Malhó, R., and Pais, M.S.S. (1992). A cytochemical study on the role of ATPases during pollen germination in *Agapanthus umbelatus* Lher. Sex. Plant Reprod. **5,** 138–145.

Feijó, J.A., Sainhas, J., Hackett, G.R., Kunkel, J.G., and Hepler, P.K. (1999). Growing pollen tubes possess a constitutive alkaline band in the clear zone and a growth-dependent acidic tip. J. Cell Biol. **144,** 483–496.

Felle, H.H. (2001). pH: Signal and messenger in plant cells. Plant Biol. **3,** 577–591.

Fricker, M.D., White, N.S., and Obermeyer, G. (1997). pH gradients are not associated with tip growth in pollen tubes of *Lilium longiflorum.* J. Cell Sci. **110,** 1729–1740.

Fu, Y., Wu, G., and Yang, Z. (2001). Rop GTPase-dependent dynamics of tip-localized F-actin controls tip growth in pollen tubes. J. Cell Biol. **152,** 1019–1032.

Ghosh, M., Song, X., Mouneimne, G., Sidani, M., Lawrence, D., and Condeelis, J. (2004). Cofilin promotes actin polymerization and defines the direction of cell motility. Science **304,** 743–746.

Gibbon, B.C., Kovar, D.R., and Staiger, C.J. (1999). Latrunculin B has different effects on pollen germination and tube growth. Plant Cell **11,** 2349–2363.

Gibbon, B.C., and Kropf, D.L. (1994). Cytosolic pH gradients associated with tip growth. Science **263,** 1419–1421.

Gluck, S., Cannon, C., and Al-Awqati, Q. (1982). Exocytosis regulates urinary acidification in turtle bladder by rapid insertion of H^+ pumps into the luminal membrane. Proc. Natl. Acad. Sci. USA **79,** 4327–4331.

Gu, Y., Fu, Y., Dowd, P., Li, S., Vernoud, V., Gilroy, S., and Yang, Z. (2005). A Rho family GTPase controls actin dynamics and tip growth via two counteracting downstream pathways in pollen tubes. J. Cell Biol. **169,** 127–138.

Guern, J., Felle, H., Mathieu, Y., and Kurkdjian, A. (1991). Regulation of intracellular pH in plant cells. Int. Rev. Cytol. **127,** 111–173.

Gungabissoon, R.A., Jiang, C.J., Drøbak, B.K., Maciver, S.K., and Hussey, P.J. (1998). Interaction of maize actin-depolymerising factor with actin and phosphoinositides and its inhibition of plant phospholipase C. Plant J. **16,** 689–696.

Harold, F.M., and Caldwell, J.H. (1990). Tips and currents: Electrobiology of apical growth. In Tip Growth in Plant and Fungal Cells, I.B. Heath, ed (London: Academic Press), pp. 59–89.

Hepler, P.K., Bosch, M., Cárdenas, L., Lovy-Wheeler, A., McKenna, S.T., Wilsen, K.L., and Kunkel, J.G. (2005). Oscillatory pollen tube growth: Imaging the underlying structures and physiological processes. Microscopy and Microanalysis **11** (suppl. 2), pp. 148–149.

Holdaway-Clarke, T.L., and Hepler, P.K. (2003). Control of pollen tube growth: Role of ion gradients and fluxes. New Phytol. **159,** 539–563.

Holdaway-Clarke, T.L., Weddle, N.M., Kim, S., Robi, A., Parris, C., Kunkel, J.G., and Hepler, P.K. (2003). Effect of extracellular calcium, pH and borate on growth oscillations in *Lilium formosanum* pollen tubes. J. Exp. Bot. **54,** 65–72.

Huang, S., Blanchoin, L., Chaudhry, F., Franklin-Tong, V.E., and Staiger, C.J. (2004). A gelsolin-like protein from *Papaver rhoeas* pollen (PrABP80) stimulates calcium-regulated severing and depolymerization of actin filaments. J. Biol. Chem. **279,** 23364–23375.

Hussey, P., Allwood, E., and Smertenko, A. (2002). Actin-binding proteins in the *Arabidopsis* genome database: Properties of functionally distinct plant actin-depolymerizing factors/cofilins. Philos. Trans. R. Soc. Lond. B Biol. Sci. **357,** 791–798.

Hwang, J., Gu, Y., Lee, Y., and Yang, Z. (2005). Oscillatory ROP GTPase activation leads the oscillatory polarized growth of pollen tubes. Mol. Biol. Cell **16,** 5385–5399.

Ketelaar, T., Allwood, E., Anthony, R., Voigt, B., Menzel, D., and Hussey, P. (2004a). The actin-interacting protein AIP1 is essential for actin organization and plant development. Curr. Biol. **14,** 145–149.

Ketelaar, T., Anthony, R.G., and Hussey, P.J. (2004b). Green fluorescent protein-mTalin causes defects in actin organization and cell expansion in Arabidopsis and inhibits actin depolymerizing factor's actin depolymerizing activity in vitro. Plant Physiol. **136,** 3990–3998.

Kost, B., Spielhofer, P., and Chua, N.H. (1998). A GFP-mouse talin fusion protein labels plant actin filaments in vivo and visualizes the actin cytoskeleton in growing pollen tubes. Plant J. **16,** 393–401.

Kovar, D.R., Drøbak, B.K., and Staiger, C.J. (2000). Maize profilin isoforms are functionally distinct. Plant Cell **12,** 583–598.

Lancelle, S.A., Callaham, D.A., and Hepler, P.K. (1986). A method for rapid freeze fixation of plant cells. Protoplasma **131,** 153–165.

Lefebvre, B., Arango, M., Oufattole, M., Crouzet, J., Purnelle, B., and Boutry, M. (2005). Identification of a *Nicotiana plumbaginifolia* plasma membrane H^+-ATPase gene expressed in the pollen tube. Plant Mol. Biol. **58,** 775–787.

Lopez, I., Anthony, R.G., Maciver, S.K., Jiang, C.J., Khan, S., Weeds, A.G., and Hussey, P.J. (1996). Pollen specific expression of maize genes encoding actin depolymerizing factor-like proteins. Proc. Natl. Acad. Sci. USA **93,** 7415–7420.

Lovy-Wheeler, A., Wilsen, K.L., Baskin, T.I., and Hepler, P.K. (2005). Enhanced fixation reveals the apical cortical fringe of actin filaments as a consistent feature of the pollen tube. Planta **221,** 95–104.

Maindonald, J., and Braun, J. (2003). Data Analysis and Graphics Using R. (Cambridge, UK: Cambridge University Press).

Messerli, M.A., Danuser, G., and Robinson, K.R. (1999). Pulsatile influxes of H^+, K^+ and Ca^{2+} lag growth pulses of *Lilium longiflorum* pollen tubes. J. Cell Sci. **112,** 1497–1509.

Messerli, M.A., and Robinson, K.R. (1998). Cytoplasmic acidification and current influx follow growth pulses of *Lilium longiflorum* pollen tubes. Plant J. **16,** 87–91.

Obermeyer, G., Lützelschwab, M., Heumann, H.G., and Weisenseel, M.H. (1992). Immunolocalization of H^+-ATPases in the plasma membrane of pollen grains and pollen tubes of *Lilium longiflorum.* Protoplasma **171,** 55–63.

Palmgren, M.G. (2001). Plant plasma membrane H^+- ATPases: Powerhouses for nutrient uptake. Annu. Rev. Plant Physiol. Plant Mol. Biol. **52,** 817–845.

Parton, R.M., Fischer, S., Malhó, R., Papasouliotis, O., Jelitto, T.C., Leonard, T., and Read, N.D. (1997). Pronounced cytoplasmic pH gradients are not required for tip growth in plant and fungal cells. J. Cell Sci. **110,** 1187–1198.

Poenie, M. (1990). Alteration of intracellular Fura-2 fluorescence by viscosity: A simple correction. Cell Calcium **11,** 85–91.

Scott, A.C., and Allen, N.S. (1999). Changes in cytosolic pH within Arabidopsis root columella cells play a key role in the early signaling pathway for root gravitropism. Plant Physiol. **121,** 1291–1298.

Sze, H., Li, X., and Palmgren, M.G. (1999). Energization of plant cell membranes by H^+-pumping ATPases: Regulation and biosynthesis. Plant Cell **11,** 677–689.

Tsai, T.D., Shuck, M.E., Thompson, D.P., Bienkowski, M.J., and Lee, K.S. (1995). Intracellular H^+ inhibits a cloned rat kidney outer medulla K^+ channel expressed in *Xenopus* oocytes. Am. J. Physiol. **268,** C1173–C1178.

Vidali, L., McKenna, S.T., and Hepler, P.K. (2001). Actin polymerization is necessary for pollen tube growth. Mol. Biol. Cell **12,** 2534–2545.

Wang, Y.S., Motes, C.M., Mohamalawari, D.R., and Blancaflor, E.B. (2004). Green fluorescent protein fusions to Arabidopsis fimbrin 1 for spatio-temporal imaging of F-actin dynamics in roots. Cell Motil. Cytoskeleton **59,** 79–93.

Wilsen, K.L., Lovy-Wheeler, A., Voigt, B., Menzel, D., Kunkel, J.G., and Hepler, P.K. (2006). Imaging the actin cytoskeleton in growing pollen tubes. Sex. Plant Reprod. **19,** 51–62.

Yokota, E., Muto, S., and Shimmen, T. (1999). Inhibitory regulation of higher plant myosin by Ca^{2+} ions. Plant Physiol. **119,** 231–239.

Yokota, E., Tominaga, M., Mabuchi, I., Tsuji, Y., Staiger, C.J., Oiwa, K., and Shimmen, T. (2005). Plant villin, lily P-135-ABP, possesses G-actin binding activity and accelerates the polymerization and depolymerization of actin in a Ca^{2+}-sensitive manner. Plant Cell Physiol. **46,** 1690–1703.